Postbuckling Analyses of Cylindrical Structures using Hybrid-Grid Systems for Derivation of Knockdown Factor

Chang Hoon Sim[*1], Jae-Sang Park*[*2] and Keejoo Lee**

Dept. of Aerospace Eng., Chungnam National Univ., Republic of Korea
[1]*sch91@cnu.ac.kr*, [2]*aerotor@cnu.ac.kr*
***Korea Aerospace Research Institute, Republic of Korea*
klee@kari.re.kr

Abstract

This work conducts the nonlinear postbuckling analyses for the stiffened cylinders for the structure of launch vehicles. Two grid systems using stiffeners -conventional orthogrid and hybrid-grid systems- are considered. The hybrid-grid systems uses two different configurations of stiffeners such as major and minor stiffeners. The single perturbation load approach is used in order to represent the initial imperfection of cylinders. A commercial finite element analysis code, ABAQUS, is used for the present nonlinear analyses. The Newton-Raphson method using displacement control scheme is applied to obtain curves of the load and the axial displacement of the stiffened cylinders under compressive loads. Through the present numerical simulations, the global and local instabilities are investigated for both stiffened cylinders using orthogrid and hybrid-grid systems. The global buckling load for a hybrid-grid cylinder is higher than that for a conventional orthogrid cylinder. In addition, the shell Knockdown factors are derived for using obtained numerical analysis results both the stiffened cylinders. Since the shell Knockdown factor of the hybrid-grid cylinder is higher than that of the conventional orthogrid cylinders, the stiffened cylinder using a hybrid-grid system is more efficient in buckling design as compared to the orthogrid cylinder.

1. Introduction

Thin cylindrical structures are used as the main element for the structure of space launch vehicles. However, they are seriously weak in buckling under axial compressive loads. Therefore, the buckling load is often considered as critical criteria in the structural design of launch vehicles. Generally, the measured buckling load in tests are much smaller than the theoretical value from a linear bifurcation buckling analysis for a geometrically perfect cylinder. This large discrepancy between tests and analyses mainly results from the initial imperfection of a cylinder. To account for this, the empirical Knockdown factor has been used in the buckling design, so that the theoretical buckling load is reduced (or knocked down) appropriately. NASA space vehicle design criteria [1] provides the lower bound of Knockdown factor with respect to various slenderness ratios (ratios of shell radius to equivalent thickness), as given in Figure 1.
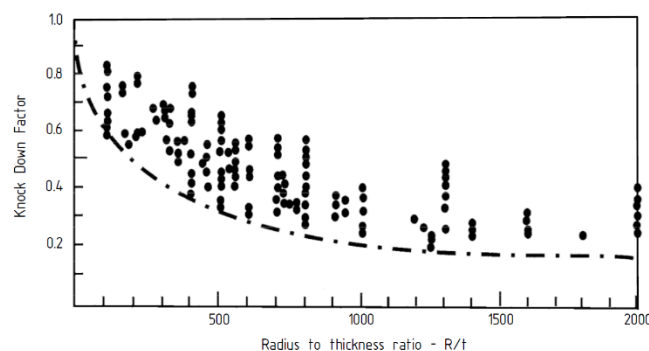

Figure 1. Lower bound of Knockdown factor

Chang Hoon Sim, Jae-Sang Park, and Keejoo Lee

This Knockdown factor is based on the collected test data from the 1930s to the 1960s; therefore, it cannot consider modern and advanced technologies for the development of launch vehicles. As a result, the design using Knockdown factors provided by NASA SP-8007 is likely to be very conservative, thus the structure is designed to be over-weighted [2]. Recently NASA's SBKF (Shell Buckling Knockdown Factor) project [3] and EU's DESICOS (New Robust DESign Guideline for Imperfection Sensitive COmposite Launcher Structures) project [4] were conducted in order to establish newly the shell Knockdown factor based on analyses to design the lightweight structure of future launch vehicles. In the two projects, the SPLA (single perturbation load approach, [5], Figure 2) was used to model the worst initial imperfection of cylinders. In the SPLA, a concentrated single perturbation load is applied in radial direction at the middle of the cylindrical structure. For both SBKF and DESICOS projects, extensive postbuckling analyses [6 - 8] as well as tests were conducted. In the numerical analyses using the finite element method, the single perturbation load is increased and a nonlinear postbuckling analysis with displacement control scheme is conducted for each lateral perturbation load. The two-step approaches are used for each lateral perturbation load as follows. In the first step, the lateral perturbation load is applied at the middle of a cylinder, and then in the second step, an axial displacement at the cylinder's end is applied while the lateral perturbation load is applied as a fixed value. This approach is repeated as the lateral perturbation load is increased until a global buckling is observed.
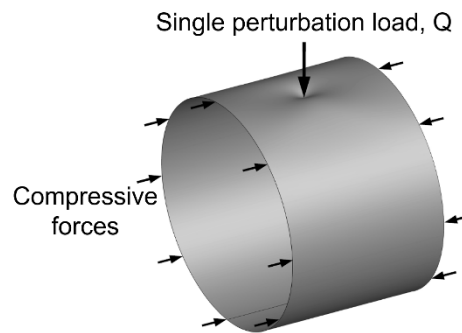

Figure 2. SPLA (Single Perturbation Load Approach) for the modeling of initial imperfection

In order to increase the stiffness and strength of cylinder to the buckling under axial compressive loads, a large number of stiffeners in the circumferential and longitudinal directions of a cylinder are used. These stiffeners are used in the forms of grids such as orthogrid and isogrid, as given in Figure 3. Generally, the configuration (shape, thickness, height, and so on) of all the stiffeners is identical in both the conventional orthogrid and isogrid systems for stiffened cylinders (Figure 4(a)). However, the hybrid-grid system (Figure 4(b)) uses two different configuration of stiffeners such as major and minor stiffeners. The major and minor stiffeners have the same cross-sectional shape (rectangle) but their cross-sectional areas (width and height) are different. This hybrid-grid system provides the reduction of the shell structural weight while buckling load is maintained or improved when the design optimization is applied [9]. Postbuckling analyses for the stiffened cylinders with hybrid-grid system were conducted partially in the reference [10], but the initial imperfection was modelled using eigenmode-shape of the cylinder.
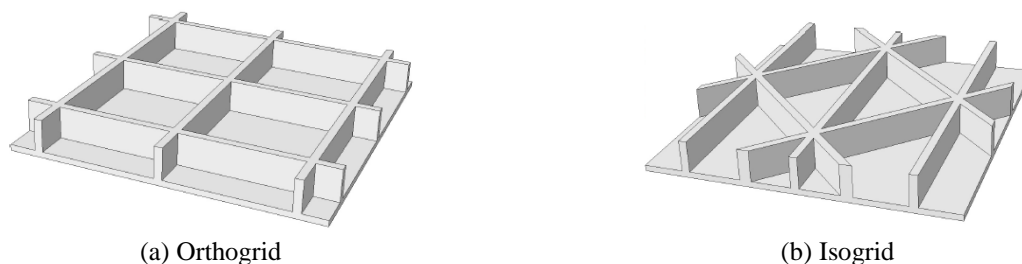

(a) Orthogrid   (b) Isogrid

Figure 3. Stiffened shells: orthogrid and isogrid systems

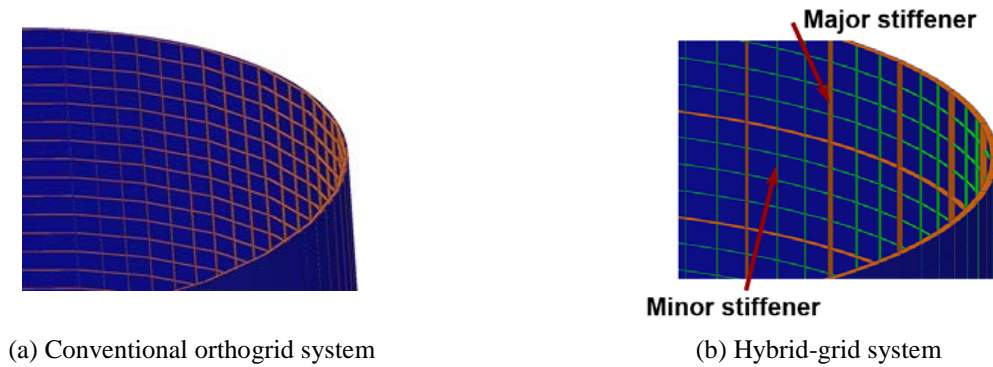(a) Conventional orthogrid system (b) Hybrid-grid system

Figure 4. Stiffened cylinders: conventional grid system (orthogrid) and hybrid-grid system

Although the stiffened cylinder using a hybrid-grid system showed that it can reduce the structural weight of space launch vehicles while the buckling load is maintained appropriately, the postbuckling analysis for it has not been conducted using the SPLA. Therefore, the present work aims to study the postbuckling analysis using the SPLA for the stiffened cylindrical structure with a hybrid-grid system. For this numerical analysis, a commercial finite element analysis code, ABAQUS (version 6.15), is used. Four node shell elements with reduced integration (S4R element) are used for the finite element analysis. The displacement control method is adopted to investigate the behaviour of the cylinder in the postbuckled state. The nonlinear static analysis with artificial damping is used to obtain the relation between the axial load and the axial displacement of a stiffened cylinder. The postbuckling analysis investigates the local and global instabilities of the cylinder using a hybrid-grid system.

Through the present study, the similarity and the difference of postbuckling behaviours of the cylinder with a conventional orthogrid system and the cylinder using a hybrid-grid system are investigated. In addition, the Knockdown factors are derived using the obtained results of numerical analyses.

2. Analytical Methods

2.1 Analysis models

The geometric parameters, boundary conditions, and material properties of the present stiffened cylinder models (orthogrid and hybrid-grid systems) are based on the stiffened cylinders used in Ref. [11]. The geometry of the present stiffened cylinders is described in Figure 5 and Table 1. The present stiffened cylinders have radius (R) of 1.5m, total length (L) of 2m and skin thickness (t_s) of 0.004m. The equally spaced stiffeners in both axial and circumferential directions are used for both grid systems. The material properties for the present stiffened cylinders are the elastic modulus of 70GPa, Poisson's ratio of 0.33, and density of 2700kg/m³.
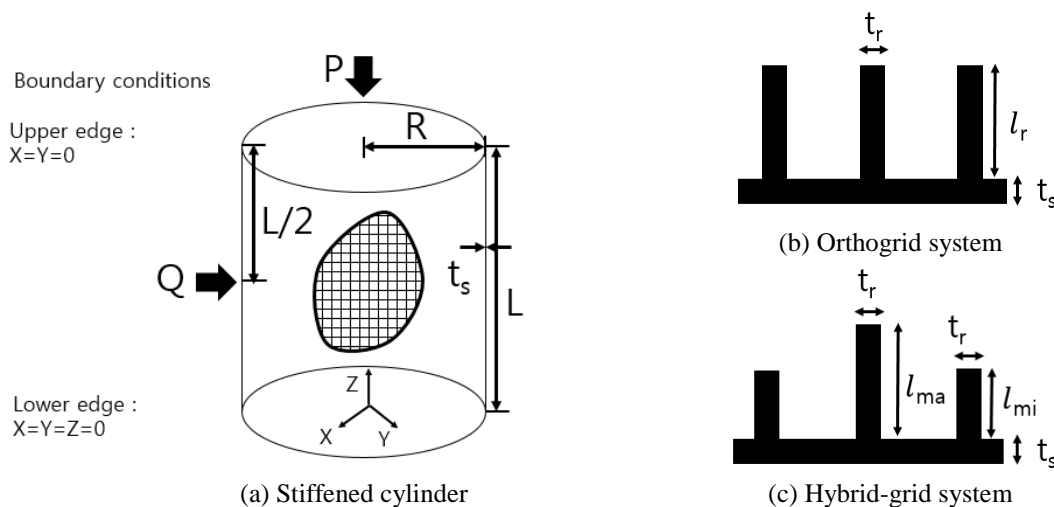

(a) Stiffened cylinder (b) Orthogrid system (c) Hybrid-grid system

Figure 5. Schematic diagrams of a stiffened cylinder and stiffeners

Chang Hoon Sim, Jae-Sang Park, and Keejoo Lee

Table 1. Geometric properties of stiffeners [11]

(a) Orthogrid system	
Stiffener thickness, t_r	0.0090 m
Stiffener length, l_r	0.0150 m
Number of circumferential stiffeners	25
Number of axial stiffeners	90
(b) Hybrid-grid system	
Minor stiffener length, l_{mi}	0.0115 m
Major stiffener length, l_{ma}	0.0230 m
Number of circumferential minor stiffeners	18
Number of axial minor stiffeners	60
Number of circumferential major stiffeners	7
Number of axial major stiffeners	30

2.2 Single perturbation load approach

The SPLA is known as one of the best methods to represent the initial imperfection of shell structures, since it can provide the realistic and worst geometric imperfection of cylindrical structures [12-15]. In the present analysis using ABAQUS, the SPLA is modelled through three-step process that is slightly different from the original modelling [16] as follows. First, a single perturbation load in radial direction is applied at the middle of the stiffened cylinder using an orthogrid or hybrid grid system in order to represent the initial imperfection of a cylinder. The application point of this lateral perturbation load is located at the intersection of a horizontal stiffener and a longitudinal stiffener (Figure 6). In this step, the nonlinear static analysis is conducted to obtain the deformed configuration of a stiffened cylinder under a lateral perturbation load. Second, the deformed shape is implemented into a perfect cylinder. This second process is for modelling of a cylinder considering the initial imperfection with stress-free, which is more realistic modelling for the initial imperfection, as compared to the original SPLA modelling [16] which is briefly summarized in Section 1. Third, the axial compressive forces are applied to the deformed stiffened cylinder but in stress-free state. In this step, the nonlinear postbuckling analysis with artificial damping is used to obtain the relation (Figure 7) between the axial load and the axial displacement of a stiffened cylinder. This process is repeated as the lateral perturbation load is increased until the global buckling load is converged.
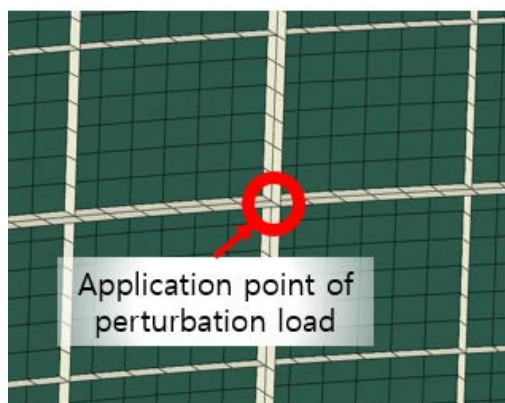

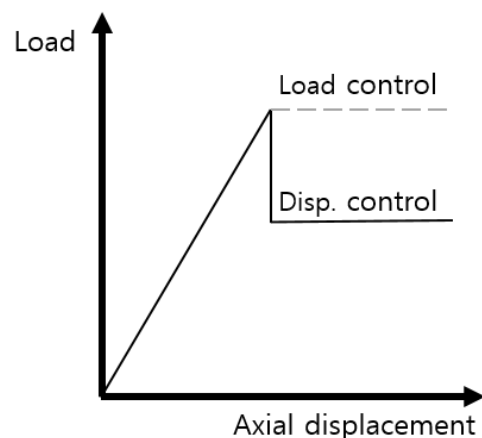Figure 6. Appilcation point of single perturbation load

Figure 7. Load – displacement curve

In the SPLA, as a single perturbation load is increased the buckling load is decreased as compared to the buckling load of a perfect cylinder without an initial imperfection (Figure 8). When the lateral perturbation load exceeds a certain perturbation load (Q_1), the buckling load is not reduced and nearly constant although the perturbation load is increased further. The corresponding buckling load is defined as the design load (N_1) of the shell structure. When the lateral

perturbation load exceeds the minimum perturbation load (Q_1) that provides constant buckling load, a small drop behaviour may be shown in the curve of load-axial displacement (Figure 9). This small drop behaviour is for the local buckling or the snap-through with a sudden radial deflection at the application point of perturbation load.
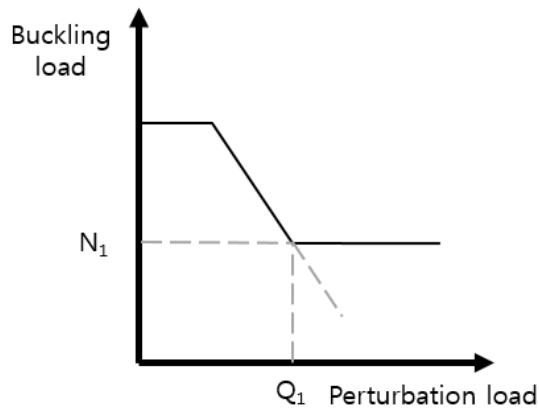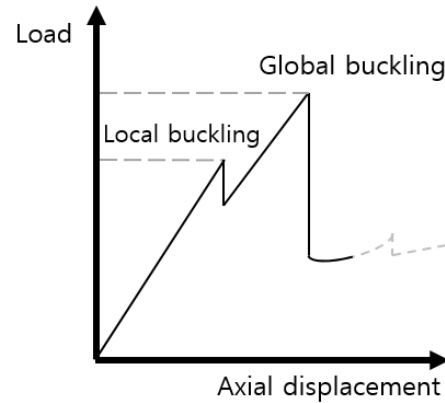

Figure 8. Buckling load vs. perturbation load

Figure 9. Global and local instabilities

2.3 Techniques for finite element modelling and analyses

Nonlinear static postbuckling analyses are performed to investigate the behaviour between load and axial displacement. The present nonlinear analyses using ABAQUS are performed using Newton-Raphson method with displacement control method. In addition, the artificial damping is applied for stabilization of the nonlinear analysis with local instability. The artificial damping dissipates the released strain energy when a local instability occurs. S4R shell elements with an element length 0.014m are used for the finite element (FE) models (Figure 10) of the present stiffened cylinders. At each end of the stiffened cylinders, nodes are coupled with a control node using rigid link (Figure 11) to apply a uniform displacement condition. The axial enforced displacement is applied to a control node to use the displacement control method. The postbuckling analyses using displacement control method may investigate the local snap-through behaviour as well as the global instability.
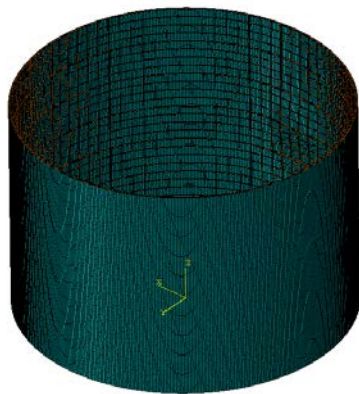
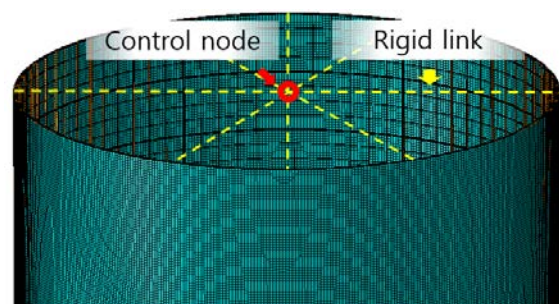

Figure 10. The ABAQS FE model of
the stiffened cylinders.

Figure 11. Rigid links and a control node

2.4 Knockdown factor

Equation (1) shows the definition of the shell knockdown factor, γ, that is a ratio between two global buckling loads of a stiffened cylinder with and without initial imperfection, $(N_{cr})_{perfect}$ and $(N_{cr})_{imperfect}$, respectively.

Chang Hoon Sim, Jae-Sang Park, and Keejoo Lee

$$\gamma = \frac{\left(N_{cr}\right)_{imperfect}}{\left(N_{cr}\right)_{perfect}} \qquad (1)$$

Therefore, the shell Knockdown factor in this paper can be defined using numerical analysis results only without test data.

3. Results of Postbuckling Analyses

3.1 Orthogrid cylinders

Figure 12 shows the result of the nonlinear static postbuckling analyses for the orthogrid cylinder. The predicted buckling load for the orthogrid cylinder without initial imperfection is 10,440kN. The behaviour between load and axial displacement is investigated by increasing the perturbation load (Q). As in the Figure 12, the global buckling load is converged to 7,532 kN. Figure 13 shows the deformed shapes as the axial load is increased while perturbation load is constant as the value of 30kN. The snap-through occurs due to local buckling caused by perturbation load (Figure 13(①)). Buckling waves spread in circumferential direction, resulting in the global buckling (Figure 13(②)). It is observed that buckling waves spread to the edge of the orthogrid cylinder as the axial load is increased further (Figure 13(③)).
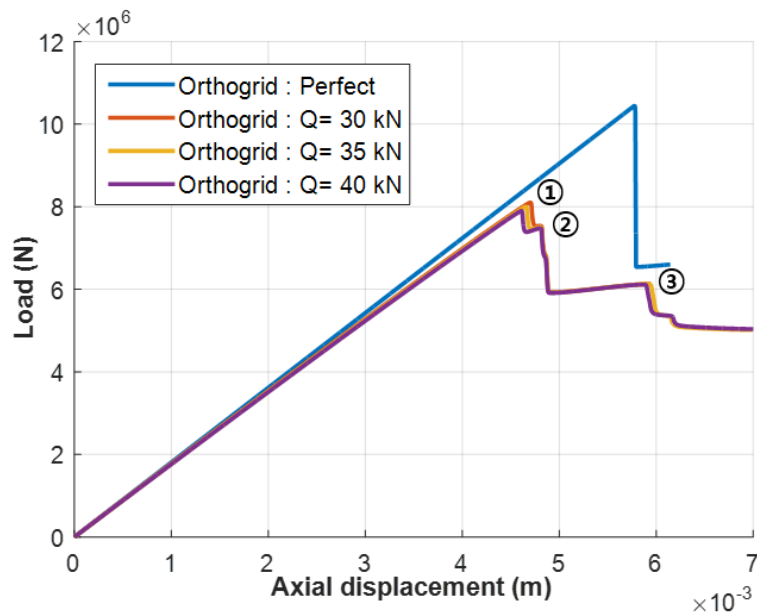

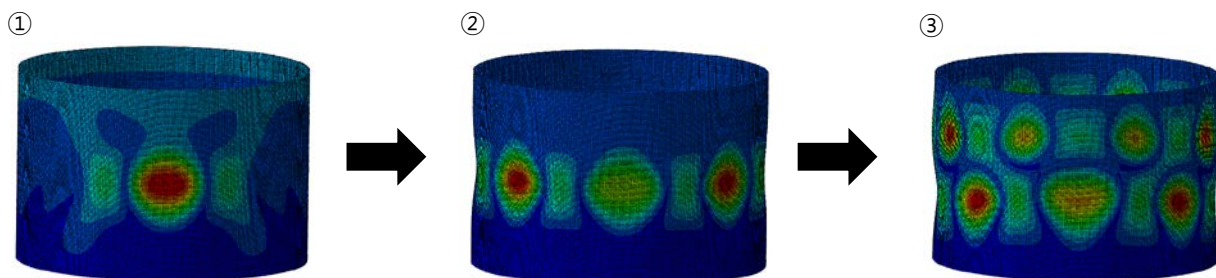Figure 12. Load – displacement curve of the orthogrid cylinder

Figure 13. Deformed shapes of the orthogrid cylinder
(lateral perturbation load Q = 30 kN)

The Knockdown factor in terms of the perturbation load is calculated using results of the present nonlinear postbuckling analyses of the orthogrid cylinder (Figure 14). As shown in Figure 14, when the lateral perturbation load exceeds 30kN, the Knockdown factor is converged to 0.72.
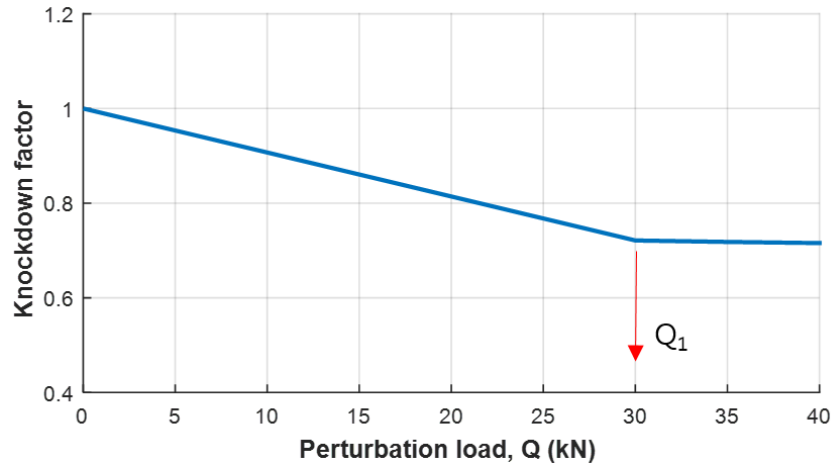

Figure 14. Knockdown factor in terms of perturbation load for the orthogrid cylinder

3.2 Hybrid-grid cylinders

The nonlinear static postbuckling analyses for the hybrid-grid cylinders were conducted in Figure 15. The calculated buckling load for the perfect hybrid-grid cylinder (without initial imperfection) is 10,580kN. The global buckling load of the hybrid-grid cylinder with initial imperfection is converged to 8,004kN as the lateral perturbation load is increased. The deformed shape of the hybrid-grid cylinder at the buckling load (8,004kN) is shown in Figure 16.
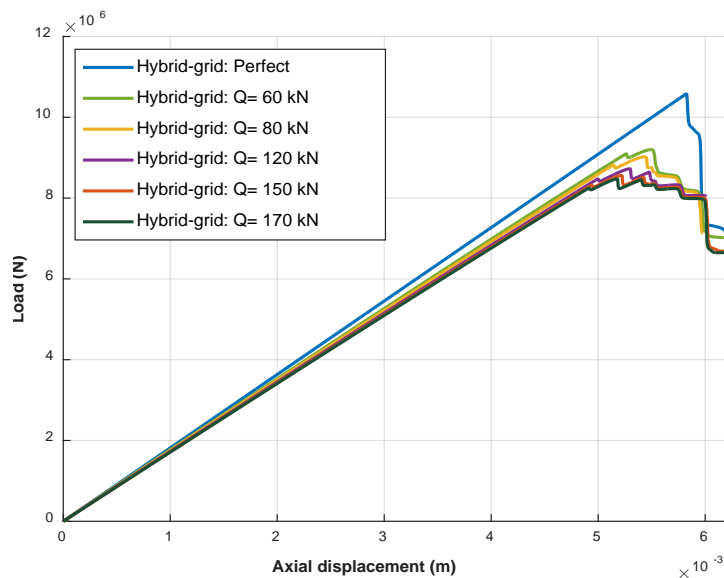

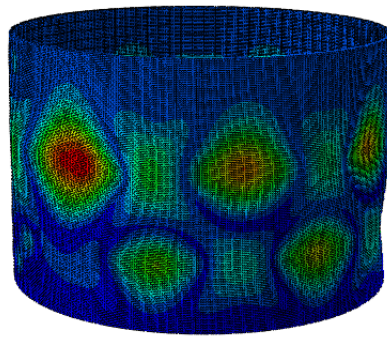Figure 15. Load – displacement curve of the hybrid-grid cylinder

Chang Hoon Sim, Jae-Sang Park, and Keejoo Lee

Figure 16. Deformed shape of the hybrid-grid cylinder
(lateral perturbation load Q = 60 kN)

Figure 15 shows the Knockdown factor of the hybrid-grid cylinder in terms of the perturbation load that is derived from the results of the present nonlinear postbuckling analyses. As shown in Figure 17, the value of Knockdown factor is converged to 0.77, when the lateral perturbation load exceeds 60kN.
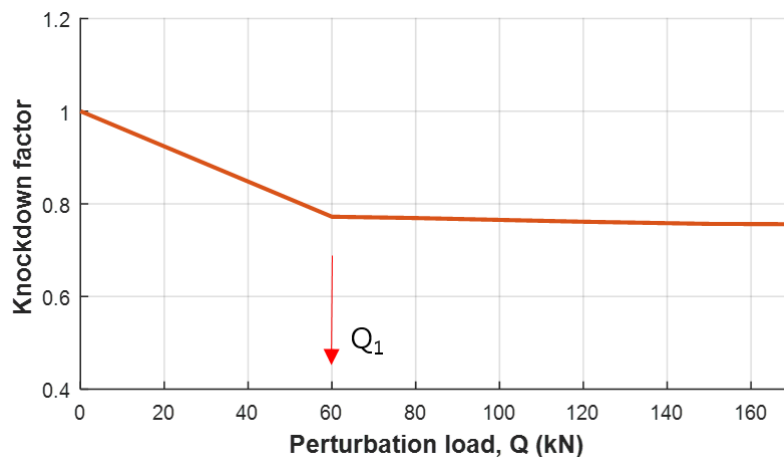

Figure 17. Knockdown factor in terms of perturbation load for the hybrid-grid cylinder

The structural weights of two stiffened cylinders are identical as the value of 354kg. As seen in Figure 12, 14, 15, and 17 the hybrid-grid cylinder is more effective to resist the buckling. In addition, since the shell Knockdown factor for the hybrid-grid cylinder is higher than that for the orthogrid cylinder, the hybrid-grid cylinder is more appropriate for the lightweight design of space launch vehicles.

4. Conclusion

This study conducted the nonlinear postbuckling analyses for two stiffened cylinders using a conventional orthogrid system and a hybrid-grid system. The single perturbation load approach was used in order to consider the initial imperfection of stiffened cylinders. ABAQUS based on the finite element method was used for this nonlinear numerical simulation. The nonlinear load-displacement relation of the stiffened cylinders under compressive loads was obtained by Newton-Rapson method with the artificial damping. In the present analyses, the local and global instabilities were observed for two stiffened cylinders. When the structural weights of two cylinders are same, the global buckling load of a hybrid-grid cylinder was higher than that of an orthogrid cylinder. Finally, the shell Knockdown factors for the orthogrid cylinder and the hybrid-grid cylinder were calculated as 0.72 and 0.77, respectively. Therefore, it can be concluded that the hybrid-grid cylinder is more efficient in buckling design from the point of view of lightweight design for space launch vehicles.

Acknowledgements

References

[1] Weingarten, V. I., Seide, P., and Peterson, J. P. 1968. Buckling of thin-walled circular cylinders. NASA SP 8007.

[2] Arbocz, J., and Starnes Jr, J. H. 2002. Future directions and challenges in shell stability analysis. *Thin-Walled Structures*, 40(9): 729-754.

[3] Hilburger, M. 2012. Developing the next generation shell buckling design factors and technologies. In: *53rd AIAA/ASME/ASCE/AHS/ASC Structures, Structural Dynamics and Materials Conference.*

[4] DESICOS Project. URL: www.desicos.eu

[5] Haynie, W., and Hilburger, M. 2010. Comparison of methods to predict lower bound buckling loads of cylinders under axial compression. In: *51st AIAA/ASME/ASCE/AHS/ASC Structures, Structural Dynamics, and Materials Conference*.

[6] Casado, V. M., Hinsch, S., Gómez, J., and Castro, G. P. 2014. Effect of initial geometrical imperfections on the buckling load of cylindrical sandwich shells under axial compression. In: *13th European conference on spacecraft structures, materials and environmental testing*.

[7] Arbelo, M. A., Degenhardt, R., Castro, S. G., and Zimmermann, R. 2014. Numerical characterization of imperfection sensitive composite structures. *Composite Structures*. 108: 295-303.

[8] Kriegesmann, B., Jansen, E. L., and Rolfes, R. 2016. Design of cylindrical shells using the single perturbation load approach–Potentials and application limits. *Thin-Walled Structures*. 108: 369-380..

[9] Hao, P., Wang, B., Li, G., Meng, Z., Tian, K., and Tang, X. 2014. Hybrid optimization of hierarchical stiffened shells based on smeared stiffener method and finite element method. *Thin-Walled Structures*. 82: 46-54.

[10] Wang, B., Hao, P., Li, G., Zhang, J. X., Du, K. F., Tian, K. and Tang, X. H. 2014. Optimum design of hierarchical stiffened shells for low imperfection sensitivity. *Acta Mechanica Sinica*. 30(3): 391-402.

[11] Hao, P., Wang, B., Li, G., Meng, Z., Tian, K., and Tang, X. 2014. Hybrid optimization of hierarchical stiffened shells based on smeared stiffener method and finite element method. *Thin-Walled Structures*. 82: 46-54.

[12] Castro, S. G., Zimmermann, R., Arbelo, M. A., and Degenhardt, R. 2013. Exploring the constancy of the global buckling load after a critical geometric imperfection level in thin-walled cylindrical shells for less conservative knock-down factors. *Thin-walled structures*. 72: 76-87.

[13] Deml, M., and Wunderlich, W. 1997. Direct evaluation of the 'worst' imperfection shape in shell buckling. *Computer methods in applied mechanics and engineering*. 149(1-4): 201-222.

[14] Haynie, W., Hilburger, M., Bogge, M., Maspoli, M., and Kriegesmann, B. 2012. Validation of lower-bound estimates for compression-loaded cylindrical shells. In: *53rd AIAA/ASME/ASCE/AHS/ASC Structures, Structural Dynamics and Materials Conference.*

[15] Castro, S. G., Zimmermann, R., Arbelo, M. A., Khakimova, R., Hilburger, M. W., and Degenhardt, R. 2014. Geometric imperfections and lower-bound methods used to calculate knock-down factors for axially compressed composite cylindrical shells. *Thin-walled structures*. 74: 118-132.

[16] Hühne, C., Rolfes, R., Breitbach, E., and Temer, J. 2008. Robust design of composite cylindrical shells under axial compression—simulation and validation. *Thin-walled structures*. 46(7): 947-962.